

# Fragmentation of the photoabsorption strength in neutral and charged metal microclusters

C. Yannouleas\* and R.A. Broglia

*Dipartimento di Fisica, Universita di Milano, and INFN, Sez. Milano, I-20133 Milano, Italy, and The Niels Bohr Institute, DK-2100 Copenhagen Ø, Denmark*

M. Brack†

*The Niels Bohr Institute, DK-2100 Copenhagen Ø, Denmark*

P.-F. Bortignon

*Istituto di Ingegneria Nucleare, CESNEF Politecnico di Milano, Italy, and INFN, LNL, Legnaro, Italy*

(Dated: 16 December 1988; Phys. Rev. Lett. **63**, 255 (1989))

The line shape of the plasma resonance in both neutral and charged small sodium clusters is calculated. The overall properties of the multipole structure observed in the photoabsorption cross section of spherical  $\text{Na}_8$  and  $\text{Na}_{20}$  neutral clusters can be understood in terms of Landau damping. Quantal configurations are shown to play an important role. In the case of charged  $\text{Na}_9^+$  and  $\text{Na}_{21}^+$  clusters a single peak is predicted that carries most of the oscillator strength.

PACS numbers: 36.40.+d, 31.50.+w, 33.20.Kf

Recent photoabsorption experiments [1] have revealed the surface plasmon in small neutral sodium clusters. A qualitative overall account of the dependence of the resonance frequencies on the cluster size can be achieved in terms of the extended ellipsoidal shell model [2, 3] and of the experimental static polarizabilities. The reported line broadening seems to obtain, as suggested in ref. [1], an important contribution from the coupling of the dipole resonance to quadrupole shape fluctuations of the cluster [4, 5].

Due to the fact that no complete photoabsorption curve has yet been experimentally determined, the detailed shapes and widths of the resonances are still rather uncertain. In particular, the contribution of direct plasmon decay mechanisms to the line widths must be investigated, especially in the case of small clusters, in view of the detailed microscopic calculations carried out by Ekardt [6] and Beck [7] within the framework of the time-dependent local density approximation (TDLA).

In the present paper, we study the structure of the plasmon resonance within the mean-field framework making use of the random phase approximation (RPA). Because these studies can most clearly be done in the case of spherical clusters, we presently restrict our analysis to the neutral  $\text{Na}_8$  and  $\text{Na}_{20}$  and to the charged  $\text{Na}_9^+$  and  $\text{Na}_{21}^+$ . It will be concluded that, in the case of the neutral  $\text{Na}_8$  and  $\text{Na}_{20}$ , Landau damping is important and that the observed line shapes are the result of a detailed interplay between quantum size effects and residual interactions among particle-hole excitations, as well as of the thermal fluctuations of the cluster shapes. In the case of the charged  $\text{Na}_9^+$  and  $\text{Na}_{21}^+$ , Landau damping is practically absent and the dipole strength essentially consists of a single peak exhausting most of the plasmon oscillator strength.

The calculations to be discussed below parallel those carried out in studies of giant resonances in nuclei (cf., i.e. [8]). A discrete particle-hole basis of dimension  $\mathcal{N}$  is constructed and the Hamiltonian

$$H = H_0 + V, \quad (1)$$

sum of the Hartree-Fock Hamiltonian  $H_0$  and the residual interaction  $V$ , is diagonalized using the RPA. In what

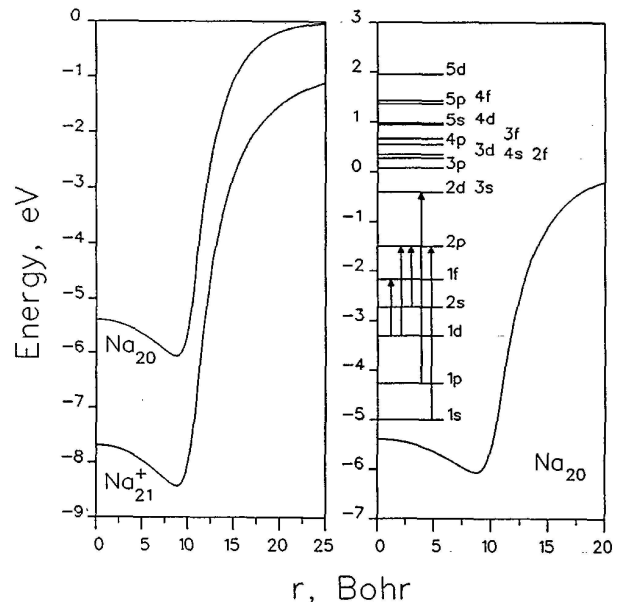


FIG. 1: Self-consistent potentials [10] associated with  $\text{Na}_{20}$  and  $\text{Na}_{21}^+$  and used in the solution of the single-particle Hamiltonian  $H_0$  appearing in eq. (1). For  $\text{Na}_{20}$ , the resulting single-particle levels relevant to the discussion of the dipole resonance, as well as some of the associated unperturbed particle-hole transitions, are also shown.

follows, we shall specify the single-particle potentials self-consistently in the spherical jellium-background model [9] using the density variational formalism in a semiclassical approximation [10]. These potentials are displayed in Fig. 1.

The residual two-body interaction  $V$  is given by

$$V(|\vec{r}_1 - \vec{r}_2|) = \frac{e^2}{|\vec{r}_1 - \vec{r}_2|} + \frac{dV_{xc}[\rho]}{d\rho} \delta(|\vec{r}_1 - \vec{r}_2|). \quad (2)$$

Here  $V_{xc}[\rho] = d\mathcal{E}_{xc}[\rho]/d\rho$  is the exchange-correlation po-

tential in the ground state. As in refs. [9, 10], we use the exchange-correlation energy density  $\mathcal{E}_{xc}[\rho]$  of Gunnarsson and Lundqvist [11].

The RPA equations (see, e.g., ref. [12])

$$\begin{pmatrix} A & B \\ B^* & A^* \end{pmatrix} \begin{pmatrix} X_n \\ Y_n \end{pmatrix} = E_n \begin{pmatrix} X_n \\ -Y_n \end{pmatrix},$$

are written in terms of the angular-momentum coupled matrix elements of the interaction (2), i.e.

$$\begin{aligned} A(ph, p'h') - (\epsilon_{n_p, l_p} - \epsilon_{n_h, l_h}) \delta_{l_p, l_{p'}} \delta_{l_h, l_{h'}} \delta_{n_p, n_{p'}} \delta_{n_h, n_{h'}} &= 2 R(ph', hp') (-)^{l_p + l_{p'}} \\ &\times \frac{[(2l_p + 1)(2l_h + 1)(2l_{p'} + 1)(2l_{h'} + 1)]^{\frac{1}{2}}}{(2\lambda + 1)} \begin{pmatrix} l_h & \lambda & l_p \\ 0 & 0 & 0 \end{pmatrix} \begin{pmatrix} l_{h'} & \lambda & l_{p'} \\ 0 & 0 & 0 \end{pmatrix} \\ &= (-)^{\lambda} B(ph, p'h'), \end{aligned} \quad (3)$$

where

$$R(ph', hp') = \int r_1^2 dr_1 r_2^2 dr_2 \mathcal{R}_{n_p, l_p}(r_1) \mathcal{R}_{n_{h'}, l_{h'}}(r_2) V(r_1, r_2; \lambda) \mathcal{R}_{n_h, l_h}(r_1) \mathcal{R}_{n_{p'}, l_{p'}}(r_2), \quad (4)$$

and where  $\mathcal{R}_{n_i, l_i}(r)$  is the radial part of single-particle wave functions. The radial contribution of the two-body interaction (2) in multipole order  $\lambda$  is given by

$$V(r_1, r_2; \lambda) = e^2 \frac{r_{<}^{\lambda}}{r_{>}^{\lambda+1}} + \frac{dV_{xc}[\rho]}{d\rho} \frac{\delta(r_1 - r_2)}{r_1^2} \frac{2\lambda + 1}{4\pi},$$

where  $r_{<} = \min(r_1, r_2)$  and  $r_{>} = \max(r_1, r_2)$ .

The indices  $n_i$  appearing in eqs. (3) and (4) denote the number of nodes for the corresponding single-particle states. The orbital angular momenta of the particles and holes participating in the excitations are denoted by  $l_i$ , the total angular momentum of the excitation being  $\lambda$ , which in the present calculation is set equal to 1 (dipole vibration). The 3j symbols appearing in (3) take proper care of the angular momentum coupling, as well as of the parity conservation conditions. The factor 2 accounts for the spin degeneracy.

The RPA eigenvectors are written as a linear combination of particle-hole excitations in terms of the forwardsgoing and backwardsgoing amplitudes,  $X_n(ph)$  and  $Y_n(ph)$  respectively, according to

$$\begin{aligned} |n\rangle &= \sum_{ph} [X_n(ph) |(ph^{-1})_{\lambda\mu}\rangle \\ &\quad - (-)^{\lambda+\mu} Y_n(ph) |(hp^{-1})_{\lambda, -\mu}\rangle], \end{aligned} \quad (5)$$

where a singlet spin configuration is implied.

The dipole transition probabilities associated with the state (5) can be written as

$$B(E1, 0 \rightarrow n) = \frac{2}{3} |\langle n | \mathcal{M}(E1) | 0 \rangle|^2,$$

where

$$\langle n | \mathcal{M}(E1) | 0 \rangle = \sum_{ph} [X_n^*(ph; 1) + (-)^{\lambda} Y_n^*(ph; 1)] \langle p | \mathcal{M}(E1) | h \rangle, \quad (6)$$

are reduced matrix elements [13] of the dipole operator  $\mathcal{M}(E1; \mu) = \sqrt{4\pi/3} e r \mathcal{Y}_{1\mu}(\hat{r})$ .

The radial wave functions  $R_{n_i, l_i}$  are calculated by diagonalizing the single-particle Hamiltonian  $H_0$  in a ba-

sis including  $\mathcal{N} = 25$  harmonic oscillator major shells. (For the oscillator parameter of this basis, we have used  $\hbar\omega = 1.1$  eV. The results do not, however, depend on this choice.)

The associated unperturbed particle-hole excitations, examples of which are displayed in Fig. 1, exhaust the Thomas-Reiche-Kuhn sum rule  $S(E1) = N\hbar^2 e^2 / 2m$ , that is

$$\sum_{ph} (\epsilon_{n_p, l_p} - \epsilon_{n_h, l_h}) |\sqrt{2/3} \langle p || \mathcal{M}(E1) || h \rangle|^2 = S(E1),$$

where  $\epsilon_{n_i, l_i}$  are the single-particle energies. This result is also valid for the correlated eigenstates (5) and associated eigenvalues  $E_n$ , since the RPA preserves the energy-weighted sum rule (EWSR).

In Fig. 2 we display the oscillator strength functions versus excitation energy for the RPA dipole in the case of the neutral  $\text{Na}_8$  and  $\text{Na}_{20}$  clusters, as well as in the case of the charged  $\text{Na}_9^+$  and  $\text{Na}_{21}^+$  clusters. The unperturbed oscillator strength for the neutral clusters is also displayed.

A conspicuous feature of the RPA results for the neutral clusters is the sizeable amount of Landau damping. In fact, the variances of these response functions are  $\sigma \approx 0.57$  eV in both cases implying a ratio  $\sigma/\bar{E} \approx 0.25$ ,  $\bar{E}$  here being the energy centroids of the resonances. Nonetheless, the identification of the collective states is quite unique. Indeed, in the case of  $\text{Na}_8$ , there is a single state at  $\approx 2.8$  eV exhausting  $\approx 75\%$  of the EWSR, while about the same strength is distributed among two lines located at 2.6 eV and 2.9 eV in the case of  $\text{Na}_{20}$ . As befitted collective states, the associated wave functions exhibit several (about ten) forwardgoing amplitudes (X-components) that are larger than 0.1. Also, most of the backwardgoing amplitudes (Y-components) contribute constructively to the transition amplitude (6). The wave functions associated with the rather weak states which are strongly red shifted with respect to the collective states are, on the other hand, dominated by a couple of components. We note that the results shown in the middle of Fig. 2 for  $\text{Na}_{20}$  display an extent of fragmentation similar to the TDLDA calculation by Ekardt (cf. Fig.6 of ref. [6]).

The plasmon strength function is drastically modified in the case of the charged  $\text{Na}_9^+$  and  $\text{Na}_{21}^+$  clusters, where a single peak lying at  $\approx 3.1$  eV ( $\text{Na}_9^+$ ) and at  $\approx 3.0$  eV ( $\text{Na}_{21}^+$ ) exhausts  $\approx 93\%$  and  $\approx 83\%$  of the EWSR, respectively. This result seems to be consistent with recent experimental findings reported[14] for the potassium clusters  $\text{K}_9^+$  and  $\text{K}_{21}^+$ .

The difference between positively charged and neutral clusters is due to the difference in the associated average potentials (cf. Fig. 1). Indeed, the potentials for the charged clusters are deeper than the potentials for the corresponding neutral clusters (observe that the potential for the neutral clusters exhibit an almost constant

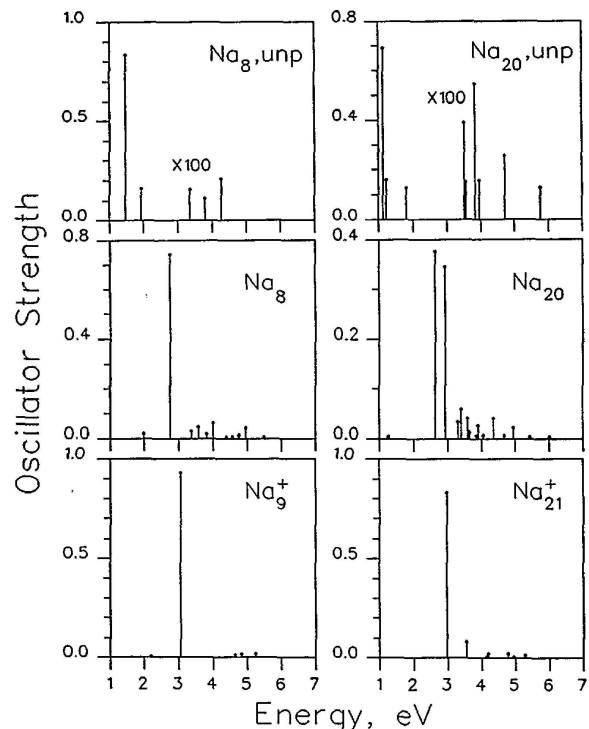


FIG. 2: Oscillator strength function for the photoabsorption of  $\text{Na}_8$ ,  $\text{Na}_{20}$ ,  $\text{Na}_9^+$ , and  $\text{Na}_{21}^+$  clusters. In the upper figures, the unperturbed oscillator strengths for the neutral clusters is displayed. Also, in the upper figures, the strength values above 3 eV have been multiplied by 100.

central depth at  $\approx -5.4$  eV). For  $\text{Na}_9^+$  the increase of the potential depth at the center amounts to  $\approx 56\%$ , while for  $\text{Na}_{21}^+$  the corresponding increase is  $\approx 42\%$ .

It is interesting to compare the moments of the dipole strength function obtained in the present microscopic RPA calculation for the case of neutral clusters with those obtained semiclassically in ref. [10]. The cubic energy-weighted sum rules and the centroids  $\bar{E}$  agree within 2 – 4%; the static dipole polarizabilities  $\alpha$  (given by the negative energy-weighted sum rules) agree within 4 – 10%. This offers support for the ability of the semiclassical method proposed in ref. [10] to predict the average properties of the mean-field response function.

In order to compare the present calculations with the experimental data, one has to take into account the coupling of the electronic dipole oscillations to thermal surface fluctuations of the whole cluster [4, 5]. This is done only for the case of neutral clusters for which the most systematic body of information is available at present[15]. In keeping with the findings of ref. [5], this can be approximately simulated by folding the peaks of the RPA spectrum with Lorentzian functions displaying a damping factor  $\Gamma/\hbar\omega_0 \approx 0.1$  and 0.06 for  $\text{Na}_8$  and  $\text{Na}_{20}$ , respectively. The results are shown in Fig. 3 in comparison with the experimental data [16]. Aside from a shift of  $\approx 10\%$ , the overall structure observed in these two cross

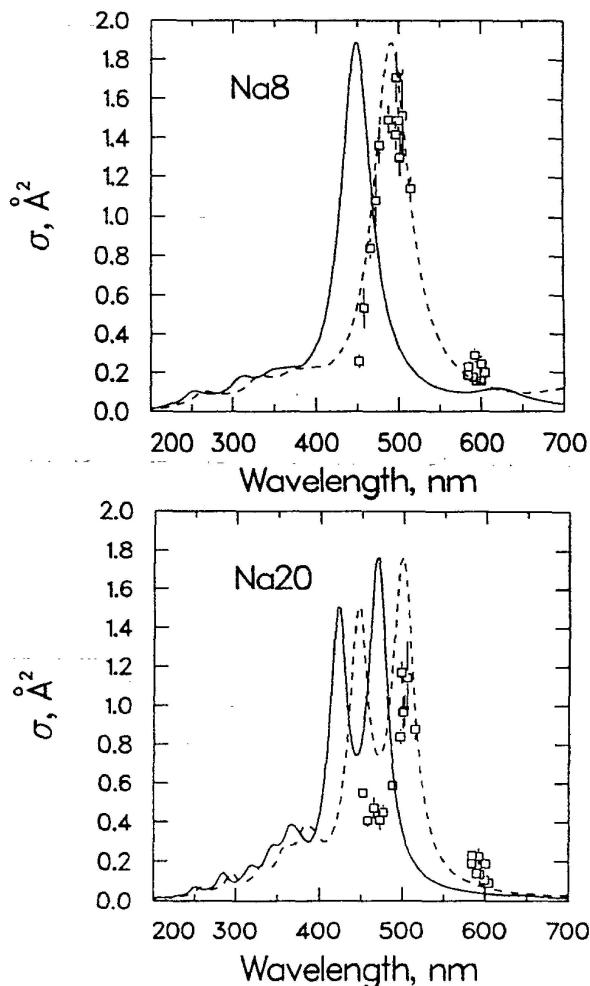


FIG. 3: Photoabsorption cross sections per atom (for  $\text{Na}_8$  and  $\text{Na}_{20}$ ) resulting from the folding of the RPA oscillator strengths with Lorentzian shapes normalized to unity are shown (solid line). The widths of the Lorentzians are specified by  $\Gamma/\hbar\omega_0 \approx 0.1$  and  $0.06$  for  $\text{Na}_8$  and  $\text{Na}_{20}$ , respectively [5],  $\hbar\omega_0$  being the peak energy of a given Lorentzian. The experimental data [16] are also shown. The dashed line is the solid line shifted so that there is a maximum overlap with the data.

sections is well reproduced. In particular for  $\text{Na}_{20}$ , the dip seen in the experimental cross section near  $460 \text{ nm}$ , as well as the weak bump in  $\text{Na}_8$  near  $590 \text{ nm}$ , seem to come out of the present RPA description.

The shift of the calculated dipole peaks with respect to the observed values for the neutral clusters is consistent with the fact that the predicted static dipole polarizabilities within the LDA model [9, 10, 17] are lower than the experimental ones by  $\approx 20\%$ . This is because the model, when applied to the exchange part of the Coulomb interaction between the electrons, provides too much screening, and thus fails to produce for neutral clusters the expected asymptotic  $1/r$  Coulomb behavior of the mean field. As a consequence, the tail of the electron densities

(the so-called 'spill-out') is underestimated; since the latter is known to be correlated to both the dipole polarizabilities [17] and the surface plasmons [10], these quantities are also underestimated. Indeed, a 'self-interaction correction' aimed at a better treatment of the Coulomb exchange within the Kohn-Sham approach [18] can improve the values for the dipole polarizabilities. It remains an open question to which extent an improved treatment of the Coulomb exchange will affect the positions of the unperturbed particle-hole excitations, and thus the detailed structures of the photoabsorption cross sections obtained in the present investigation.

It can be concluded that direct decay of the giant dipole resonance in small neutral sodium clusters plays an important role in the fragmentation of the associated strength function, a process that seems to be essentially absent in the case of the positively charged clusters. The actual location and potential fragmentation of the dipole peak in  $\text{Na}_8$  and  $\text{Na}_{20}$  is the result of a delicate balance between shell structure and residual interaction, which might be further unravelled by carrying photoabsorption measurements at low temperatures. A detailed mapping of the strongly red shifted dipole peaks and of their structure could provide some crucial tests of the exchange (plus correlation) part of the effective interaction between the electrons in metal clusters.

Discussions with W. de Heer, B.R. Mottelson and H. Nishioka are gratefully acknowledged. We wish to thank W.D. Knight and collaborators for providing us with the most recent experimental data prior to publication. One of us (C.Y.) wishes to acknowledge financial support during the course of this research from the INFN, sez. Milano, from a NATO fellowship through the Greek Ministry of National Economy, and from the Joint Institute for Heavy Ion Research, where the calculations were completed.

\* Current address: Joint Institute for Heavy Ion Research, Oak Ridge National Laboratory, Oak Ridge, Tennessee 37831.

† Permanent address: Institut für Theoretische Physik, Universität Regensburg, D-8400 Regensburg, West Germany.

- [1] W.A. de Heer et al, Phys. Rev. Lett. **59** (1987) 1805
- [2] S.G. Nilsson, Mat. Fys. Medd. Dan. Vid. Selsk. **29** (1955) no. 16
- [3] K. Clemenger, Ph. D. Thesis (Berkeley, 1985), unpublished; Phys. Rev. B **32** (1985) 1359
- [4] G.F. Bertsch and D. Tomanek, submitted to Europhysics Letters
- [5] J.M. Pacheco and R.A. Broglia, Phys. Rev. Lett. **62** (1989) 1400
- [6] W. Ekardt, Phys. Rev. B **31** (1985) 6360
- [7] D.E. Beck, Phys. Rev. B **35** (1987) 7325
- [8] N. Van Giai et al, Phys. Lett. B **199** (1987) 155; Nucl.

- Phys. A **482** (1988) 437c
- [9] W. Ekardt, Phys. Rev. B **29** (1984) 1558
- [10] M. Brack, Phys. Rev. B **39** (1989) 3533
- [11] O. Gunnarsson and B.I. Lundqvist, Phys. Rev. B **13** (1976) 4274
- [12] D.J. Rowe, Nuclear Collective Motion (Butler & Tanner, London, 1970), p. 247 ff
- [13] See, e.g., Å. Bohr and B.R. Mottelson, Nuclear Structure (Benjamin, New York, 1969), Vol. I, Sect. 1A-5
- [14] C. Bréchnignac, Ph. Cahuzac, F. Carlier, and J. Leygnier, to be published
- [15] In any case, thermal fluctuations are expected to be less important for charged clusters due to the fact that the electrons are more tightly bound, and thus the associated shell corrections[19] (Nilsson-Strutinsky model) are expected to be larger leading to a stiffer potential energy surface in the space of cluster shapes, as compared to the neutral case.
- [16] K. Selby, M. Vollmer, J. Masui, V. Kresin, M. Kruger, W.A. de Heer, and W.D. Knight, Phys. Rev. B, to be published, and Contribution, Aix-en-Provence, Meeting on Clusters, July 1988
- [17] D.E. Beck, Phys. Rev. B **30** (1984) 6935
- [18] P. Stampfli and K.H. Bennemann, Phys. Rev. A **39** (1989) 1007
- [19] M. Brack et al, Rev. Mod. Phys. **44** (1972) 320